Structural Model for Single Links of TiO_2(110)-(1×2) Surface from Analyses of Scanning Tunneling Microscopy and Density Functional Theory Calculations

Li Fengxuan (李丰烜)[1]*, Diao Zhuo (刁卓)[1], Yamashita Hayato[1],
Tohei Tetsuya[1], Abe Masayuki[1]
[1]The Osaka of University

2026 年 9 月 11 日

Abstract

Rutile TiO_2(110) is widely regarded as the prototypical metal oxide surface in surface science. For decades, the structural description of its reconstructed (1×2) link region was built upon the implicit assumption of structural symmetry, until very recent studies revealed that the (1×2) reconstruction itself is intrinsically asymmetric, rendering all earlier symmetric link region models need to be improved. Motivated by this, this work carries out a systematic reinvestigation of the link-region atomic structure through a synergistic combination of high-resolution scanning tunneling microscopy experiments and first-principles density functional theory calculations. We generate a comprehensive set of candidate models constrained by the newly confirmed asymmetric (1×2) geometry, perform full structural relaxation, and then carry out a systematic validation procedure by matching Tersoff–Hamann simulated STM images with experimental micrographs. Ultimately, this procedure yields the optimal, experimentally consistent atomic structure of the link region.

Keywords: TiO_2(110)-(1×2), STM, DFT
PACS: 07.79.Cz, 68.37.-d, 63.20.dk

1. Introduction

Titanium dioxide (TiO_2) is an important industrial material with widespread applications in catalysis, purification, and biomedicine [1–3]. Surface studies of TiO_2 are crucial for understanding its fundamental properties and optimizing its practical applications [4]. Among TiO_2 polymorphs, rutile is the most thermodynamically stable phase, with the (110) surface being particularly stable and thus serving as a prototypical model system for surface science investigations [5]. Under ultra-high vacuum (UHV) conditions, the TiO_2(110) surface initially exhibits a (1×1) structure [6]. Through repeated cycles of Ar ion sputtering and annealing, the surface exhibits modified electronic properties due to altered interactions between surface oxygen vacancies and Ti atoms, the surface undergoes reconstruction to form a (1×2) structure [7]. The (1×2) reconstructed surface shows adjusted electronic state distributions and enhanced valence band tail formation [8]. These structural modifications lead to improved photocatalytic activity and enhanced reactivity toward water molecules [7,9]. Consequently, a thorough understanding of the atomic structure and electronic properties of the (1×2) reconstruction is crucial for the development of

*Corresponding author. E-mail: 15221367061@163.com

more efficient TiO_2 catalysts. Based on previous studies, the TiO_2(110)-(1×2) surface is known to consist of two distinct structural components: the (1×2) reconstructed region and the link region [7,10]. Fig.1-a) shows an STM image acquired in this work, in which both regions can be clearly identified, consistent with the structural features reported. The structure of the (1×2) region has been extensively investigated. While a symmetric (1×2) structure was initially proposed [7], subsequent studies using density functional theory (DFT) calculations [8], scanning probe microscopy (SPM) imaging [11], and transmission electron microscopy (TEM) observations [12] have suggested that an asymmetric (1×2) structure is more plausible. Guided by these previous reports, the asymmetric structures shown in Fig.1b),c). As a result, previous models on TiO_2(110)-(1×2) surface based on symmetric (1×2) structure have to be reconsidered since the details were not so accurate based on asymmetric (1×2) structure. In addition, the link region is important because it is expected to influence catalysis and adsorption on the TiO_2(110)-(1×2) surface [13,14]. The asymmetric structure alters the uniform state in the original lattice, causing the bond lengths to elongate and the bond angles to change. The surrounding coordination has also changed, with the local coordination number and coordination atoms being adjusted, resulting in variations in the restructured area.

Previous studies have proposed different models for the link structure, including the Ti_3O_6-added-row model by Bennett et al. [15] and the more widely accepted Ti_2O_3-added-rows model [14,16]. However, neither of these two models has obtained definitive theoretical verification through DFT calculations or other equivalent theoretical research methods. Furthermore, considering the asymmetric nature of the (1×2) region, which complicates the surface situation, the link structure requires reinvestigation to achieve a more accurate structural model. In recent years, advances in DFT calculations have enabled structural validation through total energy comparisons. However, uncertainties in the atomic composition and stoichiometry of the link region make determining the optimal link structure challenging, and

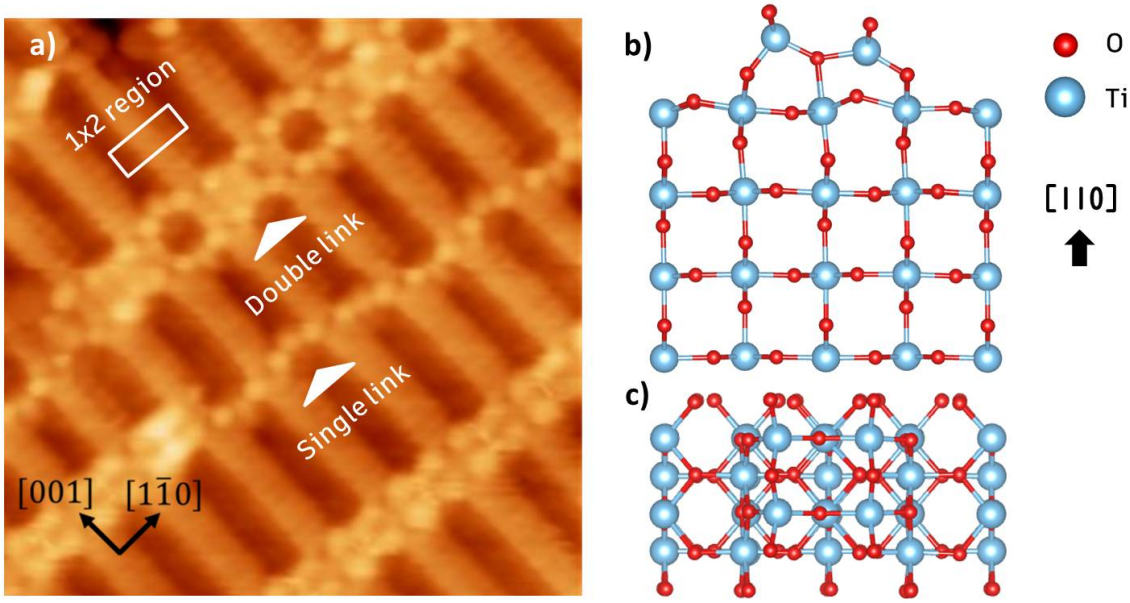


Fig. 1 a) Scanning Tunneling Microscopy (STM) image of the rutile TiO_2(110)-(1×2) surface (10 × 10 nm^2), acquired at a setpoint current $I_t = 100\,pA$ and a sample bias $V_s = 1.5\,V$. The image reveals a (1×2) reconstructed region as well as single-link and double-link structures. b) is the side view of ball-stick modeling of the asymmetric (1×2) structure and c) the top view of the asymmetric (1×2) structure.

total energy comparisons alone are not suitable for this purpose. The Tersoff-Hamann theory [17] provides a complementary approach by enabling simulation of STM images from DFT optimized structures. By directly comparing simulated STM images with experimental observations, the validity of proposed structural models can be more rigorously assessed. In this study, we combined STM observations with DFT calculations to elucidate the atomic structure of the link region on the TiO_2(110)-(1×2) surface. Based on the established asymmetric (1×2) structure, we constructed multiple candidate models for the link region and performed geometry optimization using DFT. STM images were then simulated using the Tersoff-Hamann theory for direct comparison with experimental data. Through systematic comparison of experimental and simulated STM images, complemented by energy analysis, we propose a structural model that can explain the observed link features on the TiO_2(110)-(1×2) surface.

2. Experimental and Computational Details

STM measurements were performed using a home-built STM system operating under ultra-high vacuum (UHV) conditions (<1.0×10^{-8} Pa) at room temperature. Nb-doped (0.05 wt%) rutile TiO_2(110) single crystal substrates were used. The samples were ultrasonically cleaned in ethanol before introduction into the UHV chamber. The TiO_2(110)-(1×2) reconstructed surface was prepared through repeated cycles of Ar^+ ion sputtering (1.0 keV, Ar partial pressure of 1×10^{-6} Torr, an ion current of $I = 0.4\,\mu$A, 10 min) and subsequent annealing at 900°C, starting from a clean TiO_2(110)-(1×1) surface.

DFT calculations and STM simulations were performed to investigate the link structure of the TiO_2(110)-(1×2) surface. All calculations were carried out using the Vienna Ab initio Simulation Package (VASP) [18,19]. The projector augmented wave (PAW) method was employed to describe the interaction between ions and valence electrons [19,20]. Exchange-correlation effects were treated within the generalized gradient approximation (GGA) using the Perdew-Burke-Ernzerhof (PBE) functional [21]. Partial valence potentials (*pv*) were used to include semicore states in the calculations. Structure optimization and total energy calculations were performed. The k mesh was sampled according to a Monkhorst-Pack scheme [22] with a spacing of 0.3 $Å^{-1}$. The cutoff energy in the plane wave expansion was 330 eV. Convergence of relative energies with respect to the k mesh and energy cut off was found to be better than 1 meV/atom.

STM simulations were performed using p4vasp (version 0.3.29), employing the Tersoff-Hamann theory [17]. The simulations were conducted in constant current mode with a bias voltage of +1.5 V (unoccupied states). Both structural and electronic properties required for the STM simulations were obtained from the VASP calculations.

A potential limitation of the current work is that spin polarization effects are not explicitly included in the DFT calculations. We have performed supplementary test calculations on the representative surface structure, and the results verify that spin polarization has no significant effect on simulated STM images that are concerned in this study. Nevertheless, neglecting spin polarization may still lead to minor deviations in the quantitative description of local electronic states near possible surface defects, which can be further supplemented in subsequent extended studies.

3. Results

The structural model was based on the asymmetric TiO_2(110)-(1×2) structure reported previously [12]. Despite the lack of more definitive proof, it was often assumed that the double link structure was composed

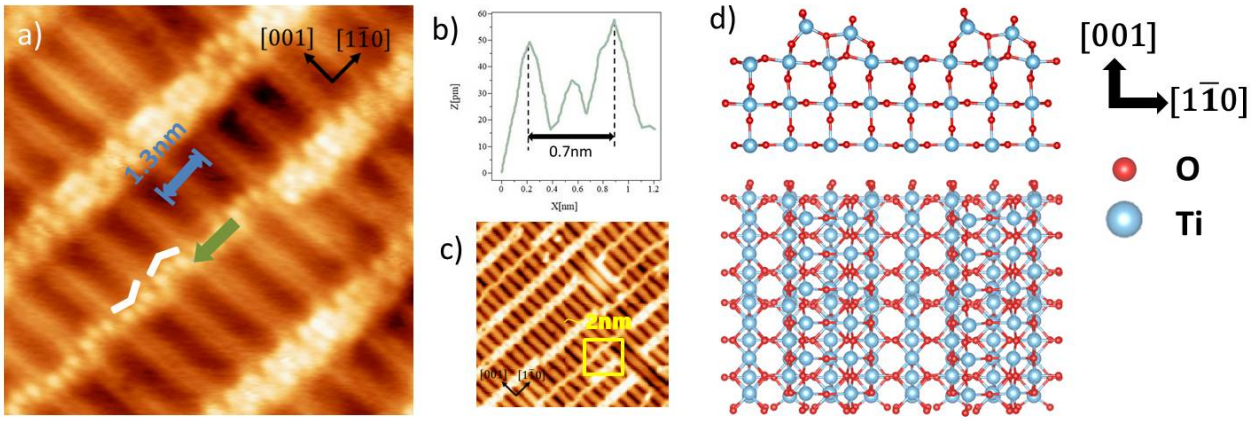


Fig. 2 a) STM image (10 nm × 10 nm) of the rutile TiO_2(110)-(1×2) surface, $I_t = 100\,pA$ and $V_s = 1.5\,V$. White arrows indicate the single links along [001] with two opposite directions, while blue arrows indicate the distance between the (1×2) columns along [1$\bar{1}$0] is 1.3 nm. b) line profile(green line) on STM image shown in a), the distance is about 0.7 nm. c) STM image(20 nm ×20 nm) of the minimum distance between links. d) the side view of the basic model of the TiO_2(110)-(1×2) surface, e) the top view of the basic model of the TiO_2(110)-(1×2) surface.

of two single link structure [14–16]. Therefore, understanding the single link structure is essential for analyzing the overall link configuration. As shown in Fig.2, through the STM image, we can get more information of the single link structure. All the single links are along [1$\bar{1}$0]. The single link has two opposite orientations along [001], which are symmetrical along [1$\bar{1}$0](white part in Fig.2-a)). Therefore, sufficient length must be reserved to verify that the direction matches the actual situation. The single link exists between two (1×2) columns and consists of roughly three equal-sized highlights. From line profile along the [1$\bar{1}$0](green line in Fig.2-a)), due to the asymmetry of the (1×2) structure, the single link may have a small height difference between the left and right side, which has roughly 0.71 nm spacing(Fig.2-b)). Although no fixed or correlated spacing between links was identified in a large number of STM images, a comparison of numerous distance values in larger-area STM images shows that the shortest observed distance is approximately 2 nm (Fig.2-c)). Therefore, the spacing between links must be at least greater than the minimum value. By considering above information obtained from experimental observations, the final model was constructed as a 2×6×1 supercell containing 492 atoms(shown in Fig.2-d)), with dimensions of approximately a=1.8 nm, b=2.6 nm, and c=2.7 nm (including about 1.5 nm vacuum layer). This supercell size was chosen to adequately represent the surface reconstruction while maintaining computational efficiency. As the test calculations showed that constraining the bottom-layer atoms had a negligible impact on the results, these atoms were fixed in all simulations.

Based on previous studies, combined with the high resolution STM images we obtained, we propose multiple models. To avoid minor structural changes caused by asymmetry, we proposed several models with different atomic numbers and structures based on the Ti_2O_3-added-rows model. The optimized structures of these modified models are illustrated in Fig.3. Due to the difference in the number of atoms, it is not practical to directly compare the total energy of different models. Although theoretically, some methods can be used for comparison, this approach is not suitable for a large number of different models. To overcome this limitation, we adopted a structure validation approach based on simulated STM images. Specifically, STM simulations were performed using the Tersoff–Hamann theory [17], which enables a

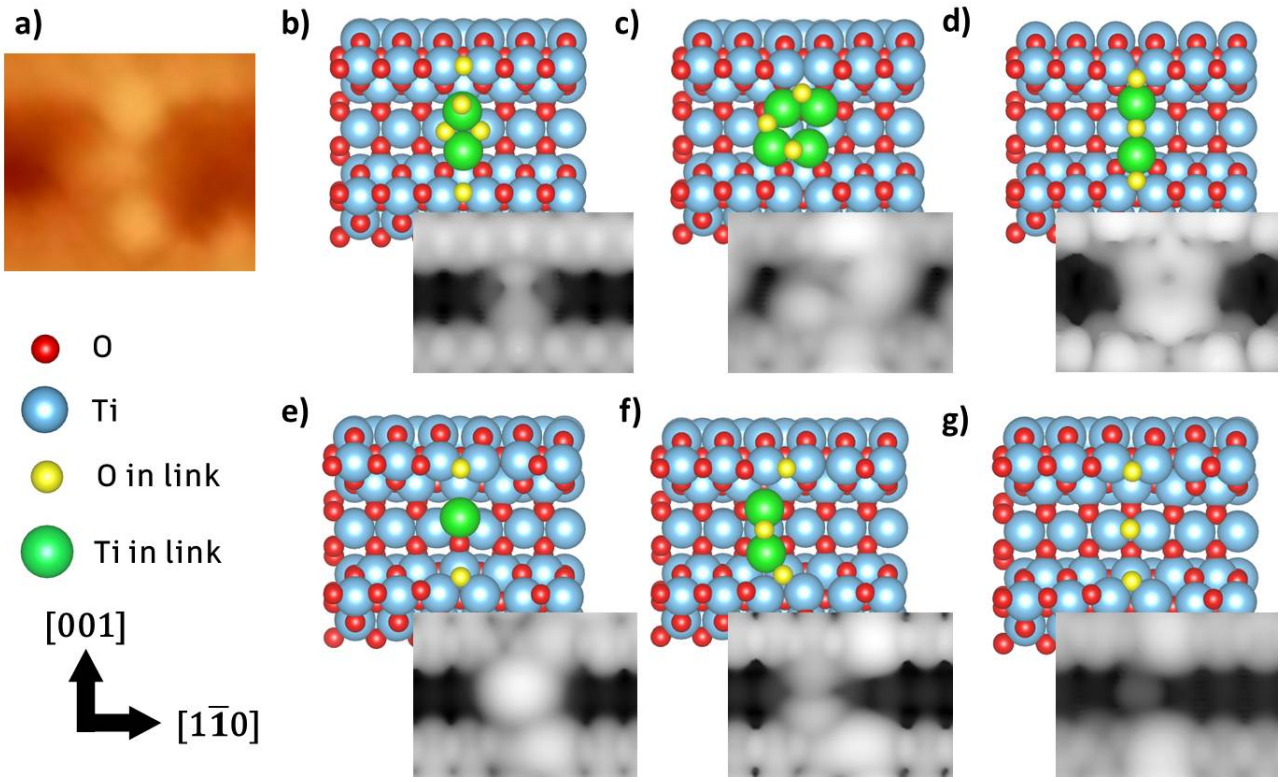


Fig. 3 Several relatively similar typical models of the link structure. a) is the STM image of the single link structure, b)-h) are the modeling of single link after optimizing and their STM simulation. b)-e) are the models of titanium atoms and oxygen atoms in different proportions based on the Ti_2O_3-added-rows model. f)-h) are the oxygen deficiency models at the bottom of the (1×2) column.)

qualitative and semi-quantitative comparison between the theoretical local density of states (LDOS) and experimentally observed STM topographies. Model validity was then evaluated by comparing the degree of agreement between the simulated and experimental STM images.

To identify the most suitable model, we examined multiple structures configurations featuring varying atomic ratios, initial positions, and arrangements. We computed approximately 50 distinct models, many of which exhibited clearly unreasonable structures, including disruptions to the (1×2) column and structural dissociation. Representative examples that closely resemble the link image were selected for presentation.

As shown in Fig.3, we considered several structural models, including the Ti_2O_3-added-rows model, variations with a similar number of atoms, models with the same link structure as the (1×2) reconstructed region, and models with reduced oxygen content. These models were structurally optimized using VASP, and the corresponding STM images were simulated.

By comparing the simulated STM images with the experimental ones, it is evident that most models in Fig. 3 deviate significantly from the experimental observations. Apart from the unconverged trial structures, we have enumerated a series of representative previously reported models in Fig. 3, which cover multiple typical sources of structural irrationality. In some cases, the link region appears notably unclear in the simulations (Fig.3-b,c,d), several damage may occur to the (1×2) region(Fig.3-c,d). while in others, the simulated link structures differ considerably from the experimental STM images and fail to reproduce the characteristic three bright spot feature (Fig.3-e,f,g).

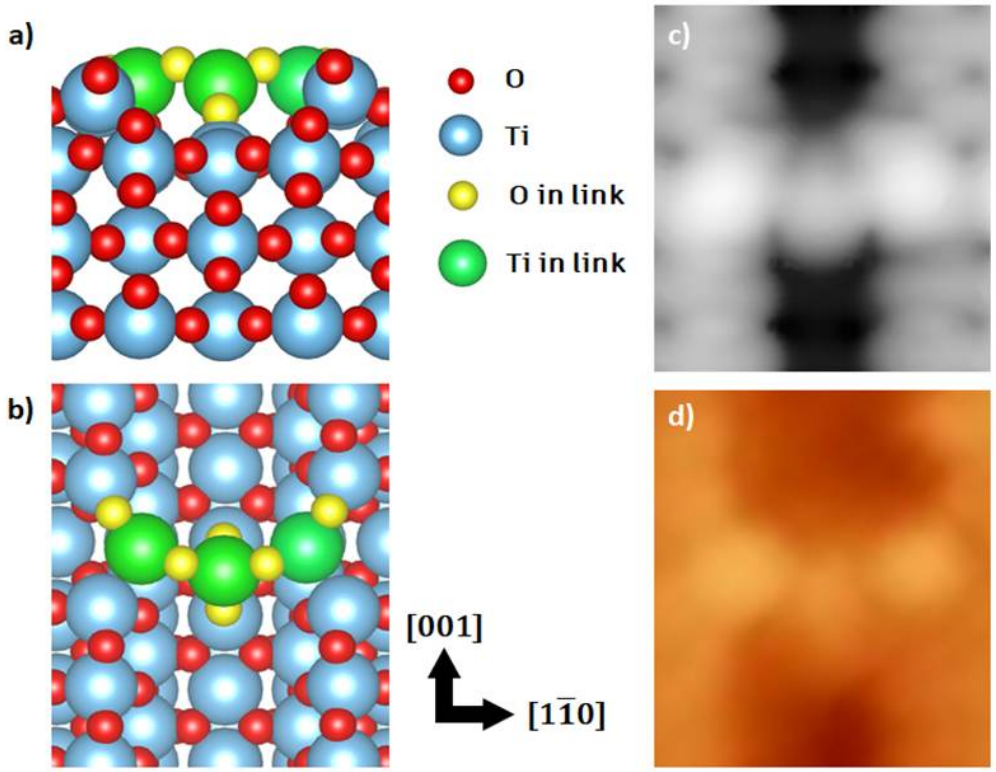
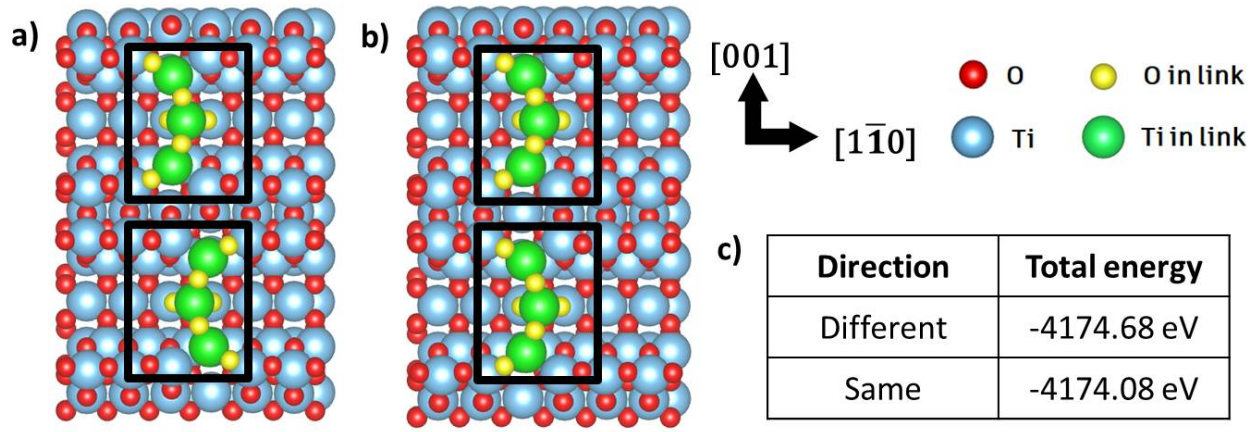


Fig. 4 Proposed (1×2) surface link structure model after optimization, a) the side view of the model(space-filling model), b) the link part on the top view of the model, c) the STM simulation of the model, d) is the STM image of single link.

In addition to the several typical structures shown in Fig.3, we also made minor adjustments to different structures for comparison. After comprehensively comparing all structures and simulations, we selected the (1×2) surface link structure model shown in Fig.4. While some of the simulated structures resemble the link structure, the structure that reproduces the three bright spots of the STM image most closely is chosen based on the structural characteristics of the link. Its overall configuration is fundamentally consistent with the Ti_2O_3-added-rows model. We further optimized this structure under asymmetric (1×2) conditions, and the results are shown in Fig.4 in comparing with experimental STM image. The distance between the bright spots in the left and right directions is approximately 0.7 nm on the STM image. And the distance between Ti atoms in the structure is 0.65 nm. The parameters of the structure also support the rationality of this model. We see good agreement between the experimental and the simulated STM image of the model.

Due to limitations in directly comparing total energy with other parameters, our primary focus is on assessing plausibility by comparing the consistency between simulated and actual images. In the STM image, we observe that single link structures exhibit opposite orientations along the [001] direction as shown in Fig.2-a). To validate this conclusion, we simulated and examined the orientation dependence of this structure, with the results shown in Fig.5. Under identical stoichiometric conditions, we conducted an energy comparison between two sets of unit cells featuring distinct chain orientations. The vacuum layer thickness in our model was set to exceed 15 Å, which could be sufficient to suppress interactions along the vertical direction. We got the relative energies of configurations with both identical and opposite orientations of adjacent single links. The results, presented in Fig.5, show that the configuration with

alternating orientations has a lower energy. This suggests that the arrangement with opposite directions is more favourable energetically and structurally, which is consistent with the features observed in the experimental STM images.



c)

Direction	Total energy
Different	-4174.68 eV
Same	-4174.08 eV

Fig. 5 Space filling model after optimizing with a) different direction of neighboring single links, b) the same direction of neighboring single links. c) is the energies of both structures. Configuration constructed in a different direction exhibits a 0.6 eV lower total energy.

4. Discussion

A comparison between the simulated images and the corresponding atomic structures indicates that the apparent height contrast in the images is inverted relative to the actual atomic height along the surface normal. This inversion suggests that the image contrast is not governed solely by geometric height, but may be influenced by differences in the local electronic structure of surface oxygen and titanium atoms. This phenomenon is consistent with previous experimental and theoretical observations on the ideal TiO_2(110) surface [23]. On the (1×1) surface, the absence of bridging oxygen atoms leads to the partial reduction of neighbouring five-coordinated titanium atoms (Ti^{5c}), resulting in the formation of localized defect states in the Ti 3d orbitals near the Fermi level, indicating electronic structure reconstruction induced by surface oxygen vacancies [24].

A similar phenomenon on the (1×2) reconstructed surface is likely related to the added-row structural model. Previous studies have shown that the formation of these states is strongly influenced by intrinsic or extrinsic defects, such as surface oxygen vacancies and subsurface titanium interstitials [25]. By correlating the local density of states features obtained from theoretical simulations with experimental scanning tunneling spectroscopy (STS) data, characteristic electronic states corresponding to specific structural motifs can in principle be distinguished. This enables a more precise identification between intrinsic surface defects and artificially constructed surface structures. Such an approach not only deepens our understanding of the electronic properties of TiO_2 surfaces, but also provides a microscopic analytical perspective for the structure-property relationship research that is essential for catalytic activity modulation.

Further DFT studies demonstrate that the LDOS distribution in rich defect regions directly impacts the adsorption energies of catalytic intermediates, thereby altering reaction pathways and kinetics [26]. Therefore, LDOS features extracted from DFT simulations can serve as structural descriptors for further studies. This not only provides theoretical support for understanding TiO_2, but also opens new avenues

for the rational design of related functional surface structures.

5. Conclusion

This study combines STM and DFT simulations to investigate the single link on the TiO_2(110)-(1×2) reconstruction surface based on asymmetric (1×2) structure. By comparing STM simulation images with actual STM images, based on previous studies [12,14], we validate a single model based on asymmetric (1×2) structure among verified models. Also, we compared the states at different alignments by comparing the total energy, and the results obtained are consistent with those of the STM images.

6. Acknowledge

This work was supported by use the Grant-in-Aid for Scientific Research number 22K18945.

参考文献

[1] FB Li and XZ Li. The enhancement of photodegradation efficiency using pt–tio_2 catalyst. *Chemosphere*, 48(10):1103–1111, 2002.

[2] Tsuyoshi Ochiai and Akira Fujishima. Photoelectrochemical properties of tio_2 photocatalyst and its applications for environmental purification. *Journal of Photochemistry and photobiology C: Photochemistry reviews*, 13(4):247–262, 2012.

[3] Sevda Jafari, Baharak Mahyad, Hadi Hashemzadeh, Sajjad Janfaza, Tooba Gholikhani, and Lobat Tayebi. Biomedical applications of tio_2 nanostructures: recent advances. *International journal of nanomedicine*, pages 3447–3470, 2020.

[4] Shalini Reghunath, Dephan Pinheiro, and Sunaja Devi KR. A review of hierarchical nanostructures of tio_2: Advances and applications. *Applied Surface Science Advances*, 3:100063, 2021.

[5] Ulrike Diebold. Structure and properties of tio_2surfaces: a brief review. *Applied physics A*, 76(5):681–687, 2003.

[6] Ulrike Diebold. The surface science of titanium dioxide. *Surface science reports*, 48(5-8):53–229, 2003.

[7] Hiroshi Onishi and Yasuhiro Iwasawa. Reconstruction of tio_2(110) surface: Stm study with atomic-scale resolution. *Surface science*, 313(1-2):L783–L789, 1994.

[8] Qinggao Wang, Artem R Oganov, Qiang Zhu, and Xiang-Feng Zhou. New reconstructions of the (110) surface of rutile tio_2 predicted by an evolutionary method. *Physical review letters*, 113(26):266101, 2014.

[9] PW Murray, NG Condon, and G Thornton. Effect of stoichiometry on the structure of tio_2(110). *Physical Review B*, 51(16):10989, 1995.

[10] María Blanco-Rey, José Abad, Celia Rogero, Javier Méndez, María Francisca López, José A Martín-Gago, and PL de Andres. Structure of rutile tio_2(110)-(1× 2): formation of ti_2o_3 quasi-1d metallic chains. *Physical review letters*, 96(5):055502, 2006.

[11] Daiki Katsube, Shoki Ojima, Eiichi Inami, and Masayuki Abe. Atomic-resolution imaging of rutile tio$_2$(110)-(1× 2) reconstructed surface by non-contact atomic force microscopy. *Beilstein Journal of Nanotechnology*, 11(1):443–449, 2020.

[12] Wentao Yuan, Bingwei Chen, Zhong-Kang Han, Ruiyang You, Ying Jiang, Rui Qi, Guanxing Li, Hanglong Wu, Maria Veronica Ganduglia-Pirovano, and Yong Wang. Direct in-situ insights into the asymmetric surface reconstruction of rutile tio2 (110). *Nature Communications*, 15(1):1616, 2024.

[13] Yaobiao Xia, Ke Zhu, Zhenrong Zhang, and Kenneth Park. Photo-stimulated desorption of trimethyl acetic acid on cross-linked (1× 2) tio$_2$(1 1 0) probed by scanning tunneling microscopy. *Applied Surface Science*, 511:145553, 2020.

[14] Satoru Takakusagi, Ken-ichi Fukui, Fumito Nariyuki, and Yasuhiro Iwasawa. Stm study on structures of two kinds of wide strands formed on tio2 (110). *Surface science*, 523(1-2):L41–L46, 2003.

[15] RA Bennett, P Stone, NJ Price, and M Bowker. Two (1× 2) reconstructions of tio$_2$(110): surface rearrangement and reactivity studied using elevated temperature scanning tunneling microscopy. *Physical review letters*, 82(19):3831, 1999.

[16] Ken-ichi Fukui and Motoyoshi Sakai. Formation of one-dimensional c60 rows on tio$_2$(110)-1× 2-cross-link structure and their local polymerization. *The Journal of Physical Chemistry B*, 110(42):21118–21123, 2006.

[17] Jerry Tersoff and Donald R Hamann. Theory of the scanning tunneling microscope. *Physical Review B*, 31(2):805, 1985.

[18] Georg Kresse and Jürgen Furthmüller. Efficient iterative schemes for ab initio total-energy calculations using a plane-wave basis set. *Physical review B*, 54(16):11169, 1996.

[19] Georg Kresse and Daniel Joubert. From ultrasoft pseudopotentials to the projector augmented-wave method. *Physical review b*, 59(3):1758, 1999.

[20] Peter E Blöchl. Projector augmented-wave method. *Physical review B*, 50(24):17953, 1994.

[21] John P Perdew, Kieron Burke, and Matthias Ernzerhof. Generalized gradient approximation made simple. *Physical review letters*, 77(18):3865, 1996.

[22] Hendrik J Monkhorst and James D Pack. Special points for brillouin-zone integrations. *Physical review B*, 13(12):5188, 1976.

[23] Hatice Ünal, Ersen Mete, and Sinasi Ellialtıoglu. Re-assigning (1× 2) reconstruction of rutile tio$_2$(110) from dft+ u calculations. *arXiv preprint arXiv:1104.3072*, 2011.

[24] PG Moses, Anderson Janotti, Cesare Franchini, Georg Kresse, and Chris G Van de Walle. Donor defects and small polarons on the tio$_2$(110) surface. *Journal of Applied Physics*, 119(18), 2016.

[25] María Blanco-Rey, J Abad, Celia Rogero, Javier Méndez, María Francisca López, E Román, José A Martín-Gago, and PL de Andrés. Leed-iv study of the rutile tio$_2$(110)-1× 2 surface with a ti-interstitial added-row reconstruction. *Physical Review B—Condensed Matter and Materials Physics*, 75(8):081402, 2007.

[26] S Funk and U Burghaus. Adsorption of co_2 on oxidized, defected, hydrogen and oxygen covered rutile (1×1)-$tio_2(110)$. *Physical Chemistry Chemical Physics*, 8(41):4805–4813, 2006.